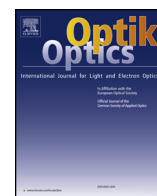




Contents lists available at ScienceDirect

Optik

journal homepage: www.elsevier.com/locate/ijleo

Original research article

Detail enhancement of infrared image based on bi-exponential edge preserving smoother

Yitong Li, Ning Liu*, Ji Xu, Jinzhi Wu

Nanjing University of Posts and Telecommunications, College of Electronic and Optical Engineering & College of Microelectronics, 9 Wenyuan Ave., Nanjing, Jiangsu Province, 210023, China

ARTICLE INFO

Keywords:

Infrared image
Detail enhancement
Bi-exponential edge-preserving filter
Gray-scale remapping
Dynamic range compression

ABSTRACT

In this paper, a new infrared image detail enhancement algorithm has been raised. The original infrared image has a wide dynamic range of 12- or 14-bit. This suppresses the human observation range of 8-bit. Usually the original infrared image needs to be compressed and gray-scale remapped for displaying. However, the normal way of doing this cannot give a better visual effect for the human observer. In this case, detail enhancement algorithms of infrared image occur. Modern detail enhancement algorithms can extract the detail information from an original infrared image and separate the image into different layers, and each layer will be processed with different strategy. Although good performance has been proved for these algorithms, there are still certain deficits such as too much computational time, low working efficiency, hard application flexibility and so on. Under this circumstances, we propose this new algorithm to overcome these problems. This algorithm uses a two dimensional convolution to separate the detail information from an original infrared image, and turn the original image into the detail layer and the base layer. The detail information will be enhanced without any unwanted artifacts. During the detail extraction, We speed up the whole computational process by transforming the two dimensional convolution into two one dimensional convolutions, and then express the one dimensional convolution with the iterative computation. After adding the enhanced detail layer back to the histogram equalized base layer, the visual quality of the original image can be improved. This algorithm not only gives better detail enhancement performance, but also reduces the computational time. Figures and data tests show the priority of our suggestions.

1. Introduction

Infrared imaging has been applied to many industrial, civilian and military fields for so many years. Modern high-quality infrared thermal imagers display images in a wide dynamic range. Usually the raw sensor outputs digital signal within 12- or 14-bit range. However, human observer can distinguish only about 128 level of gray scale in an image [1]. Thus, the raw infrared images need to be processed into the suitable display range. Many histogram equalization (HE) algorithms can done the job above [2–6], these HE algorithms usually compress the whole gray scale of a raw infrared image into the full 8-bit display range. The contrast of the infrared image will be re-mapped in order to illustrate more scenarios for human observer. But these HE algorithms somehow have certain deficits, for example, they might produce significant noise. In this case, several modified HE algorithms occur such as the contrast limited adaptive histogram equalization (CLAHE) [7]. This algorithm has more flexibility in choosing the local histogram mapping

* Corresponding author.

E-mail address: coolboy006@sohu.com (N. Liu).

<https://doi.org/10.1016/j.ijleo.2019.163300>

Received 21 December 2018; Received in revised form 16 June 2019; Accepted 26 August 2019
0030-4026/ © 2019 Elsevier GmbH. All rights reserved.

function, by selecting the clipping level of the histogram, undesired noise amplification can be reduced. In summary, these HE-based methods could compress the dynamic range of a raw infrared image into satisfied observation range, however, they lack flexibility in manipulating small details of the raw image since they are based on only the histogram information, which makes the histogram equalization algorithm cannot fully illustrate the detail within the infrared image. Ergo, many kinds of detail enhancement methods have been raised to lift the dynamic range of the raw infrared images.

Modern detail enhancement algorithms usually process the raw infrared in the following thoughts: Consider the raw infrared image is composed by two parts which are the detail layer and the base layer. The detail layer contains high frequency information while the base layer contains the histogram information. After the separation of the image, the detail layer will be enhanced by certain ways, while the base layer will be histogram equalized, then the two processed layers will be added back to form a new image. This new image is well detail enhanced for the observer. The most important thing in this process structure is that the edge-preserving filter has great ability to distinguish image detail from the noise. To our knowledge, the image detail and the noise of an image are both the high frequency information, which means that, during the separation, the noise might be mixed into the detail layer and enhanced as well. If this happens, the image quality of the final result will be degraded. So the edge-preserving filter has to be carefully chosen. In 2011, Zuo et al proposed a method using the bilateral filter to deal with the image [8,16,17]. The bilateral filter is a very good non-linear edge-preserving filter, this method gives an inspiration to the later researcher. But the bilateral filter has certain deficits, for example, since it has the feature of non-linearity, it will produce the gradient reverse effect which causes the “ghost effect” at the strong edge position of an infrared image. In 2014, we proposed a method using the guided image filter to modify the processing procedure [9,18]. We consider that the guided image filter is a linear filter, thus the gradient reverse effect will not occur. The results proved our assumption. But as it is a linear filter, the guided image filter cannot distinguish the detail and the noise as effective as the bilateral filter. We kept on our working and to the year 2016, we proposed a new method with the modified bilateral filter called the joint-bilateral filter to enhance the image details [10]. The joint-bilateral filter uses two adjacent images to compute the detail information, compare to the normal bilateral filter, the gradient reverse effect is well suppressed. Also, it has good detail separation performance. At the meantime, we discover some problems of these detail enhancement algorithms when we apply them to the real equipment. The most depressing aspect is that the complex computation of these edge-preserving filters takes too much calculation time for real-time realization. This happens not only in the software programming on the PCs or laptops, but also when migrates the algorithm into the FPGAs. Although we have done significant job to realize both these algorithms into real-time system with the hardware description language, the on-chip logic elements of the FPGA are much occupied and the power consumption is hard to lower down. Meanwhile, these filters have several parameters for the users to adjust, which means that, the realization of self-adaptive is almost mission impossible.

Based on the deep study of the infrared thermal imager, we figure out that, since the total response model can be described as a bi-exponential statistical fitting model [11], we propose a new detail enhancement algorithm in this paper with the Bi-Exponential Edge Preserving Smoother (BEEPS). The BEEPS is raised by Philippe Thevenaz et al. for filtering image noise [12]. We have made modification for BEEPS to make it well adapt to infrared image. The new proposed algorithm has the advantage of very fast and easy calculation, the improvement of the computational time is in orders of magnitude. Besides, it also has the advantage of easy application. It must be point out that, the calculation of this new algorithm only concerns about the dimension of the input image, and has nothing to do with neither the image data nor the parameters, not even the degrade of filtering.

The structure of this paper is organized as follows: in section II, the detailed theory of this new algorithm is demonstrated; in section III, the experimental results and the results comparison with other algorithms are demonstrated; in section IV, we give conclusion of our work.

2. Basic theory of our research

2.1. Brief of our idea

In Section 2, we will fully introduce our new infrared image detail enhancement algorithm. The whole processing procedure can be described as the following flow chart:

As shown in Fig. 1, the original infrared image will be first filtered by the BEEPS, since the BEEPS is used to smooth a image, we reverse the computation by subtracting the filtered result from the original image, then the detail layer can be acquired [13]. The detail layer contains most of the high frequency information, as we mentioned above, noise might be mixed into the detail layer, so we have to carefully tune the filter parameters to avoid the noise and enhance the details. The filtered result can be recognized as the base layer which contains most of the energy of the image. That is to say, the contrast of the image is determined by the base layer. According to the nature that the infrared image has high dynamic range, the base layer needs to be compressed using histogram equalization method. After processing on both layers separately, we add these two layers back together to form a new processed image [14]. The brief steps of this algorithm is described as follows:

- 1 Input an original 14- or 16-bit raw infrared image.
- 2 Conduct the BEEPS onto the raw infrared image, and the image will be filtered into detail layer and base layer.
- 3 The detail layer will be enhanced by controlling the key parameters and the gain coefficients to reach a satisfied level.
- 4 The base layer will be histogram equalized to compress the gray scale of the raw image into 8-bit display range, here, a simple accumulative histogram equalization method will do.
- 5 After combining the enhanced detail layer and the histogram equalized base layer back together, we can get an improved image

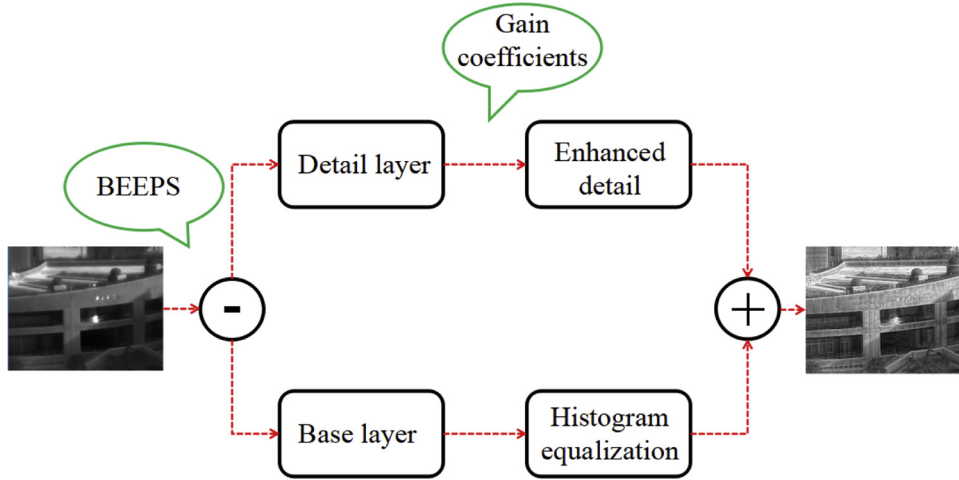


Fig. 1. The processing flow chart of our algorithm.

with good visual effect.

Next, we will give specific discussions about how the BEEPS works and how the key parameters affect the final detail enhancement performance.

2.2. Basic theory of BEEPS

The BEEPS is a kind of the non-linear filter [12,15]. To our knowledge, the general low pass filters such as the Gaussian filter only concern about the spatial region, while the non-linear filter concern about both the spatial and the range region. If two adjacent pixel value which belong to a strong edge are quickly changed, the Gaussian filter cannot distinguish this kind of changing and the edge then cannot be preserved. Usually in the normal bilateral filter [8], two kernels are used in calculating the spatial filtering and the range filtering, if a strong edge is detected, the spatial filtering will affect the range filtering by a certain decay of the value in the range kernel, which makes the range filter preserving the edge. While in BEEPS, it concentrates on both the spatial and range region too. The main difference is that, the BEEPS separates the two-dimensional non-linear filtering into two one-dimensional progressive computation process. This not only simplifies the calculation, but also maintains the performance of the detail extraction, which makes the BEEPS very useful.

The BEEPS algorithm consists of a pair of one-tap recursions. r represents a range filter. The parameter λ controls the degree of smoothing of a convolutional space filter with impulse responses. The first recursion is progressive, and $x[k]$ is the current sample of an input sequence x at location k . We can recursively compute the elements of an auxiliary sequence as eq.1:

$$\phi[k] = (1 - \rho[k]\lambda)x[k] + \rho[k]\lambda\phi[k + 1] \quad (1)$$

Where

$$\rho[k] = r(x[k], \phi[k + 1]) \quad (2)$$

The second recursion is regressive and very similar to the first one, except for a reversal of the order in which the indices are traversed. We recursively compute a second auxiliary sequence as:

$$\varphi[k] = (1 - \vartheta[k]\lambda)x[k] + \vartheta[k]\lambda\varphi[k - 1] \quad (3)$$

Where

$$\vartheta[k] = r(x[k], \varphi[k - 1]) \quad (4)$$

The BEEPS can be computed by merging the resulting progressive sequence and regressive sequence to produce the samples of the output sequence as:

$$y[k] = \frac{\varphi[k] - (1 - \lambda)x[k] + \phi[k]}{1 + \lambda} \quad (5)$$

For general use of BEEPS, the smoothing parameter λ is often choosing between $[0,1]$, although r can be chosen freely, it is customary to assume that it takes the shape of a centered bump function. In particular, a prototypical instance is the de-normalized Gaussian function. Here we choose r as the following Gaussian function:

$$r(u, v) = e^{-\frac{(u-v)^2}{2\sigma^2}} \quad (6)$$

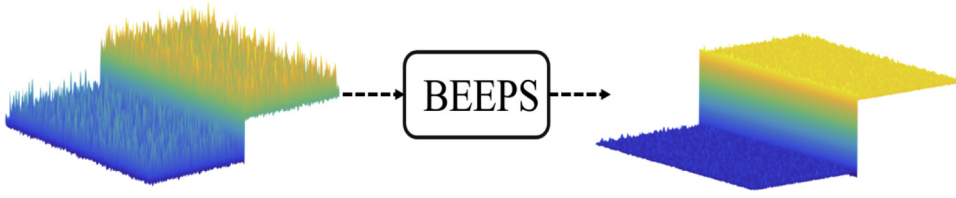


Fig. 2. The smoothing effect of BEEPS.

The standard deviation σ represents the width of the chosen bump function. When a strong edge occurs, the σ restrains the smoothing effect along with λ in order to preserve the edge. It has to be point out that, the calculation of BEEPS needs no convolution to participate, which means that, unlike the bilateral filter and the guided image filter, the BEEPS is way much faster than them. The filtering effect is simulated as the following Fig. 2:

As we mentioned above, BEEPS preserves the edges as good as the bilateral filter. This can be seen from Fig. 2, at the adjacent region of a strong edge, the BEEPS will not destroy or blur the shape of edge while filter the high frequency information away from the edge. By correctly selecting the parameter λ and σ , the BEEPS can effectively distinguish noise from the high frequency details. Next, we give demonstration on how these two parameters working on smoothing the images, or in other words, extracting the details.

By expanding the recursions, Eq. (1) and Eq. (3) can be rewritten in a way that conceals the explicit dependence of $\varphi[k]$ on $\varphi[k-1]$ and of $\phi[k]$ on $\phi[k+1]$, then these two equations are shown as follows:

$$\varphi[k] = \sum_{n=1}^{\infty} \left(\prod_{p=0}^{n-1} \vartheta[k-p] \right) (1 - \vartheta[k-n]\lambda^n x[k-n] + (1 - \vartheta[k]\lambda)x[k]) \quad (7)$$

$$\phi[k] = \sum_{n=1}^{\infty} \left(\prod_{p=0}^{n-1} \rho[k+p] \right) (1 - \vartheta[k+n]\lambda^n x[k+n] + (1 - \rho[k]\lambda)x[k]) \quad (8)$$

Then, the output Eq. (5) of BEEPS can be rewritten in the next form:

$$\begin{aligned} y[k] &= \frac{\vartheta[k](1 - \vartheta[k-1]\lambda)}{1 + \lambda} \lambda x[k-1] + \frac{1 - \vartheta[k]\lambda}{1 + \lambda} x[k] \\ &\quad \frac{\rho[k](1 - \rho[k+1]\lambda)}{1 + \lambda} \lambda x[k+1] + \frac{1 - \rho[k]\lambda}{1 + \lambda} x[k] \\ &\quad - \Lambda x[k] + O(\lambda^2) \\ &= \underbrace{\frac{\vartheta[k]\lambda}{1 + \lambda}}_{a_p} x[k-1] + \underbrace{\frac{\rho[k]\lambda}{1 + \lambda}}_{a_R} x[k+1] + \underbrace{\left(1 - \frac{(\vartheta[k] + \rho[k])\lambda}{1 + \lambda} \right)}_a x[k] + O(\lambda^2) \end{aligned} \quad (9)$$

Where, $\Lambda = \frac{1-\lambda}{1+\lambda}$ is the normalize factor of λ . We can use the same strategy to rewrite the normal bilateral filter into the form like Eq. (9), and it goes like:

$$\begin{aligned} o[k] &= \underbrace{\frac{r_{k,k-1}\lambda}{r_{k,k+1}\lambda + r_{k,k} + r_{k,k-1}\lambda + O(\lambda^2)}}_{a_{0p}} x[k-1] \\ &\quad + \underbrace{\frac{r_{k,k}}{r_{k,k+1}\lambda + r_{k,k} + r_{k,k-1}\lambda + O(\lambda^2)}}_{a_0} x[k] \\ &\quad + \underbrace{\frac{r_{k,k+1}\lambda}{r_{k,k+1}\lambda + r_{k,k} + r_{k,k-1}\lambda + O(\lambda^2)}}_{a_{0R}} x[k+1] + O(\lambda^2) \end{aligned} \quad (10)$$

Comparing Eq. (9) and Eq. (10), we calculate the limitation of the respective terms and get the following results:

$$\begin{aligned} \lim_{\lambda \rightarrow 0} \frac{a_p}{a_{0p}} &= \frac{r(x[k], \varphi[k-1])}{r(x[k], x[k-1])} \\ \lim_{\lambda \rightarrow 0} \frac{a}{a_0} &= 1 \\ \lim_{\lambda \rightarrow 0} \frac{a_R}{a_{0R}} &= \frac{r(x[k], \phi[k+1])}{r(x[k], x[k+1])} \end{aligned} \quad (11)$$

We can see from Eq. (11), once the value of λ set to 0, all three limitations with Eq. (11) have the same results and equal to 1, in

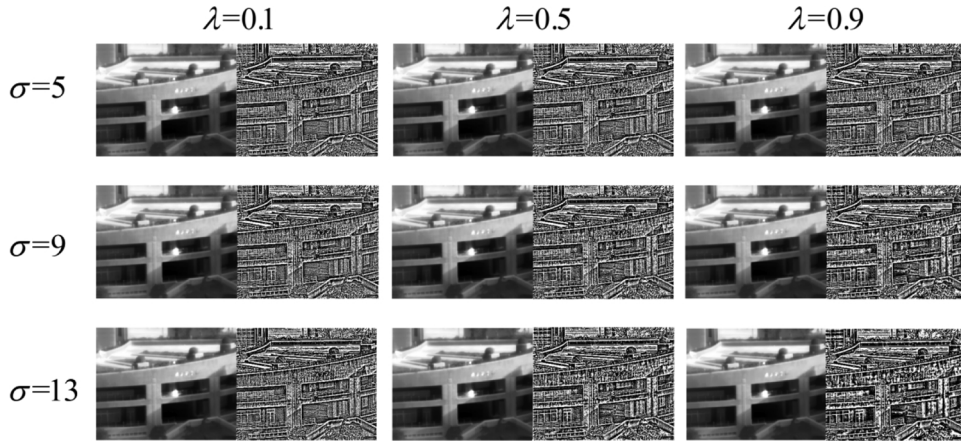


Fig. 3. Parameter performance of BEEPS on smoothing images.

this case, the BEEPS has the same form of the normal bilateral filter. That is why the BEEPS can maintain the edge preserving performance as the bilateral filter. In the real application, the value of λ will not be set as 0, we usually choose it within $[0,1]$. That means, the BEEPS has its own advantage in preserving the edge.

Next, we show a figure on different value of λ and σ affects the filtering performance.

It can be seen from Fig. 3 that, the parameters λ and σ work hand in hand to affect the filtering result. According to the former analysis, λ is a smoothing parameter, while σ is a ranging parameter. Here we explain more about these two parameters. Since the BEEPS has the character of recursion computation, the eq.1 and eq.3 need to be initialized as follows:

$$\begin{aligned}\varphi[0] &= x[0] \\ \phi[k-1] &= x[k-1]\end{aligned}\tag{12}$$

When the calculation starts, the BEEPS will initialize the two recursive term, then during the process on the input image, λ works in the special region of an image, and determines whether a strong edge or a detail information is encountered. Here we have to point out, the BEEPS not only extracts the edge information, but also details in the adjacent pixels which highly changed in gray values. If λ is chosen bigger, more detail information will be spot out and categorized into the detail layer, otherwise, less detail information will be spot out. Fig. 3 proves that when $\lambda = 0.9$, the detail extraction is better than when $\lambda = 0.1$ and $\lambda = 0.5$. However, a problem occurs when extracting the detail with BEEPS, that is, the noise problem. Only with the effect of λ is not sufficient to distinguish noise from the details, so the work of σ begins. σ is the standard deviation of the range filter r , it determines whether an edge or detail spot out by the parameter λ can be categorized into the detail layer. When pixels are in a non-edge region, the σ in the bump function of r helps the iterate the Eqs. (1) and (3). While in the edge region between indices $(k-1)$ and k , the σ will reinitialize $\phi[k]$ and $\varphi[k]$ before the recursion is resumed. So the total computation speed of BEEPS is way much faster than other edge-preserving algorithms. In real application, if σ is chosen bigger, the noise will be eliminated from the detail. In Fig. 3, when we choose $\sigma = 13$ and $\lambda = 0.9$, we can see that, the detail information appeals to be the best, and the noise is hardly seen. Next, we give clear demonstration of our whole processing procedure with this pair of parameters as follows:

It can be seen from Fig. 4 that, the processed image has been enhanced the details, meanwhile, the gray scale of the original image has been mapped into a much satisfied level. Neither too bright nor too dark region exists in the image. The enhanced detail in Fig. 4(c) appears extremely clear. More sophisticated analysis and comparison of our new algorithm and the former raised methods will be demonstrated in the next section.

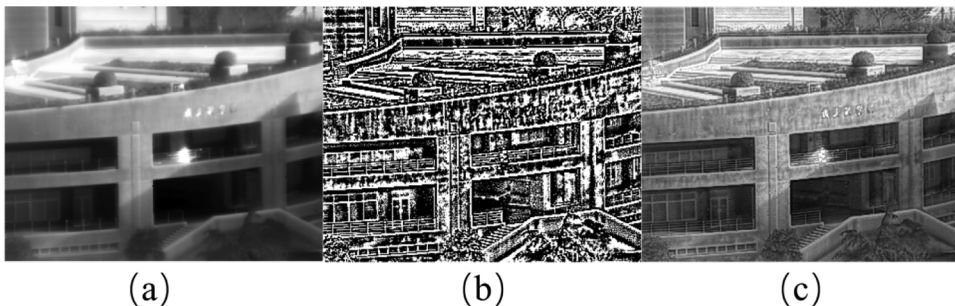


Fig. 4. The processing result of our new algorithm. (a) the original histogram equalized infrared image; (b) the detail extraction; (c) the final result of our algorithm.

2.3. Histogram equalization process of the base layer

The BEEPS separates the raw infrared image into the detail layer and the base layer. The detail layer is enhanced during the separation according to the parameters σ and λ , while the base layer which directly concerns about the contrast of the processed image has to be processed by the histogram equalization in order to compress the raw image into 8-bit range for human observation. Here we briefly give the main procedure of the histogram equalization in our method.

We binarize the base layer with a threshold T . The number of pixels of the total gray level in the raw infrared image will be considered as valid when it surpasses T , otherwise it will be considered as invalid. This identification can be written in the following equation:

$$H(x) = \begin{cases} 0, & n_x < T \\ 1, & n_x \geq T \end{cases} \quad (13)$$

Where, n_x is the number of pixels with the same gray level x . In Eq. (13), we use the threshold T to control the total contrast of the processed image. Then, we can get the cumulative distribution of the raw image written in the following equation:

$$D(x) = \begin{cases} 0, & x = 0 \\ \frac{\sum_{y=0}^{x-1} H(y)}{n_{\text{valid}}}, & \text{other} \end{cases} \quad (14)$$

After this, the base layer can be mapped into the dynamic range R :

$$R = \min(n_{\text{valid}}, D) \quad (15)$$

Here, n_{valid} is the total number of the indicated valid gray values, and D is the display range of a normal 8-bit monitor. If the dynamic range of the raw image is not high enough, the output range should not be mapped because if we do so, the final image will look very dark and noisy. The valid gray level could be a very small value. If this happens, the equalization process should be adjusted as eq.16 to make it good:

$$I_{BP} = \frac{(D - R)}{P} + D[I_B] * R \quad (16)$$

In eq.16, I_{BP} is the mapped base layer, I_B is the original base layer with less valid gray levels. P is a parameter for tuning the brightness. We can see that, the adjusted base layer projection will not be dark when modifying the factor $\frac{(D - R)}{P}$ into a high value.

3. Analysis and comparison

In this section, we will give clear demonstration of the performance of our new algorithm in infrared image detail enhancement. The test platform is a laptop with Intel i7-4710 processor. We will compare the performance through 3 aspects: the visual effect, the computational time and the background variation-detail variation (BV-DV) index. We use 4 edge-preserving filters to process all 5 infrared images and compare the results, which are the bilateral filter method, the guided image filter method, the joint-bilateral filter method and our new method [9–11]. According to Fig. 1, the edge-preserving filters extract the detail layer, while the base layer needs to be histogram equalized. We set the same mapping threshold to conduct the histogram equalization in order to compare the detail extracting and enhancing performance only. The experimental results are objective.

3.1. Visual effect comparison

In the first test set, we can see that, the new algorithm clearly has the best processing performance. Since we use the same threshold to conduct the histogram equalization onto the base layer, the final performance of these 4 methods can be judged all by the effect of each edge-preserving filter. Let us take a look at the colored boxes in Fig. 5(b)-(e), in the yellow boxes, there are five Chinese characters on the walls. Fig. 5(a) shows that, these characters cannot be recognized by the human observer. After the detail enhancement, they can be distinguished. The bilateral filter, joint bilateral filter and our new method perform better than the guided image filter, which proves that non-linear filter has the advantage of extracting details than the linear filter. Although the bilateral filter, joint-bilateral filter and the BEEPS are all belong to the non-linear filter, these are still differences. Also in the yellow boxes, clearly the detail looks much obvious in Fig. 5(e) than in Fig. 5(b)-(d). At the meantime, let us take a look at the red boxes in Fig. 5(b)-(e), the performance appears even more unanimous. The dark region spot by the red boxes in Fig. 5(b) and Fig. 5(d) is still dark, but this time, the guided image filter gives a better enhancement to this region. However, it does not compare to the performance of our new algorithm. We can see from Fig. 5(e), the contents in the dark region can be seen clearly. Finally, the scenario in Fig. 5(e) has been processed better, no matter the roof of the building, the tree leaves, windows, bars, an so on.

In Fig. 6, we can see that, in the original image, we cannot tell the mountain far away, the bilateral filter, the joint-bilateral filter and guided image filter can show us something, but with our new algorithm, the mountain shows its whole face. Also we can see from the red boxes, the details on the building are all showed up out of the shadow. One other thing is that, the contrast is better with the BEEPS than the other methods, which makes the processed image look much satisfier and much real.

In Fig. 7, the region in the red boxes are parts of the mountain, the performance with our new algorithm is better than the other

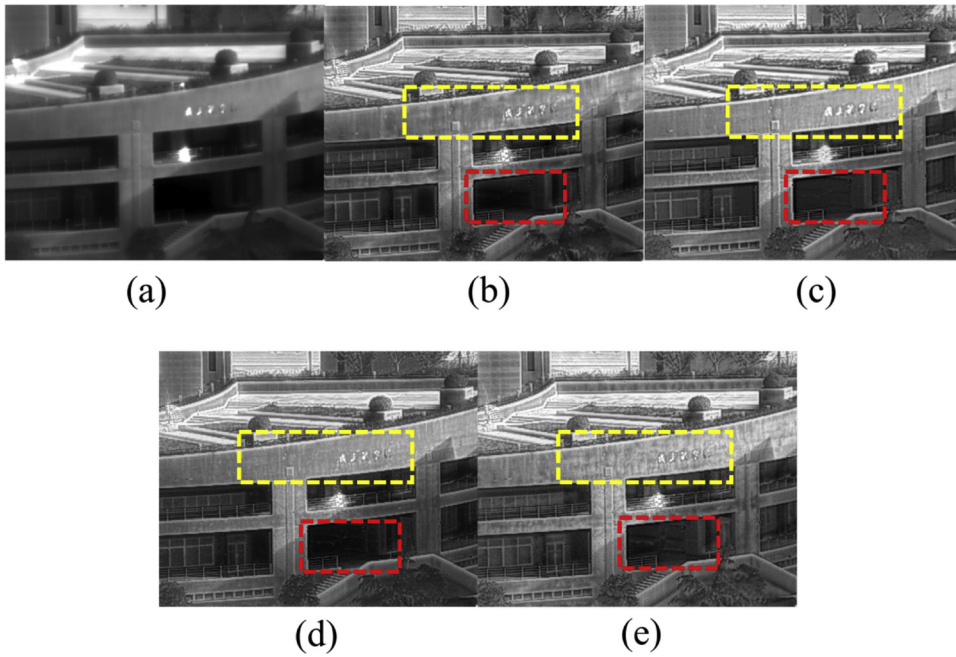


Fig. 5. Test set 1 of the enhancing performance. (a)the original image with normal histogram equalization; (b)detail enhancement with the bilateral filter; (c)detail enhancement with the guided image filter; (d)detail enhancement with the joint-bilateral filter; (e)detail enhancement of our new algorithm with BEEPS.

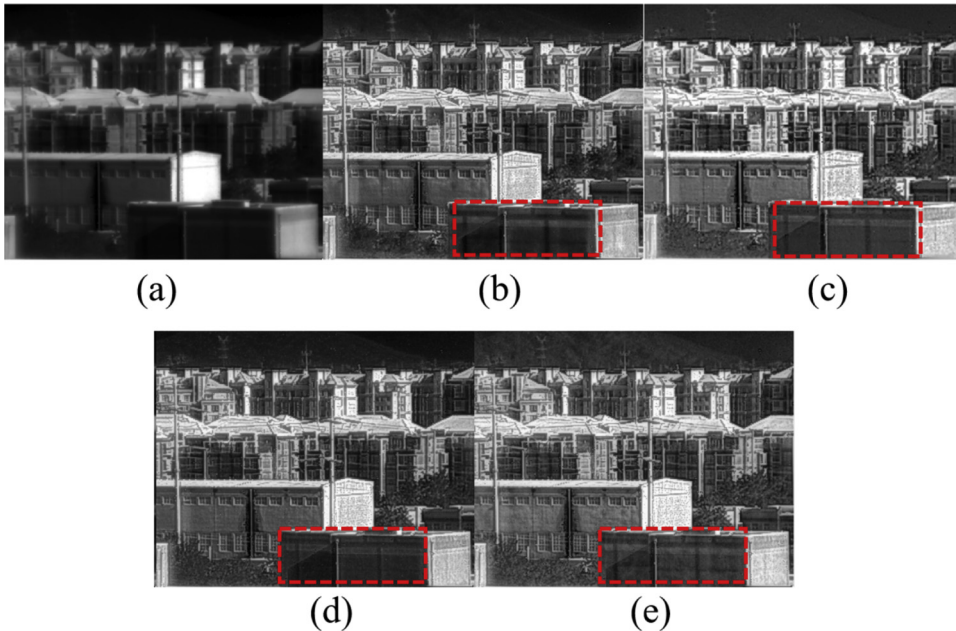


Fig. 6. Test set 2 of the enhancing performance. (a)the original image with normal histogram equalization; (b)detail enhancement with the bilateral filter; (c)detail enhancement with the guided image filter; (d)detail enhancement with the joint-bilateral filter; (e)detail enhancement of our new algorithm with BEEPS.

three. Also in the yellow boxes, the leaves appear much clearer with our new method.

In Fig. 8, we choose an image with extremely high temperature object in it. The solder iron has the temperature up to almost 400°C, such high temperature compresses the histogram of the original image into an extreme way, no background object can be seen under this situation. After filtering with these 4 method, the detail has been extended and one lamp showed up. It is clearly that, our algorithm is better than the others. The lamp in Fig. 7(e) is brought out the dark most. Meanwhile, the detail of muscle and vein in the

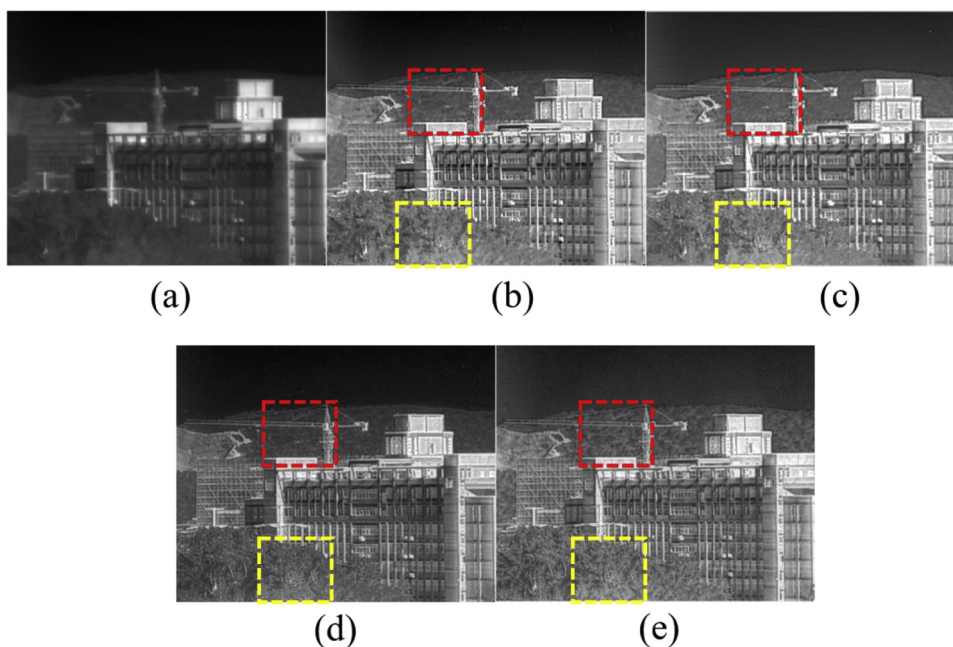


Fig. 7. Test set 3 of the enhancing performance. (a)the original image with normal histogram equalization; (b)detail enhancement with the bilateral filter; (c)detail enhancement with the guided image filter; (d)detail enhancement with the joint-bilateral filter; (e)detail enhancement of our new algorithm with BEEPS.

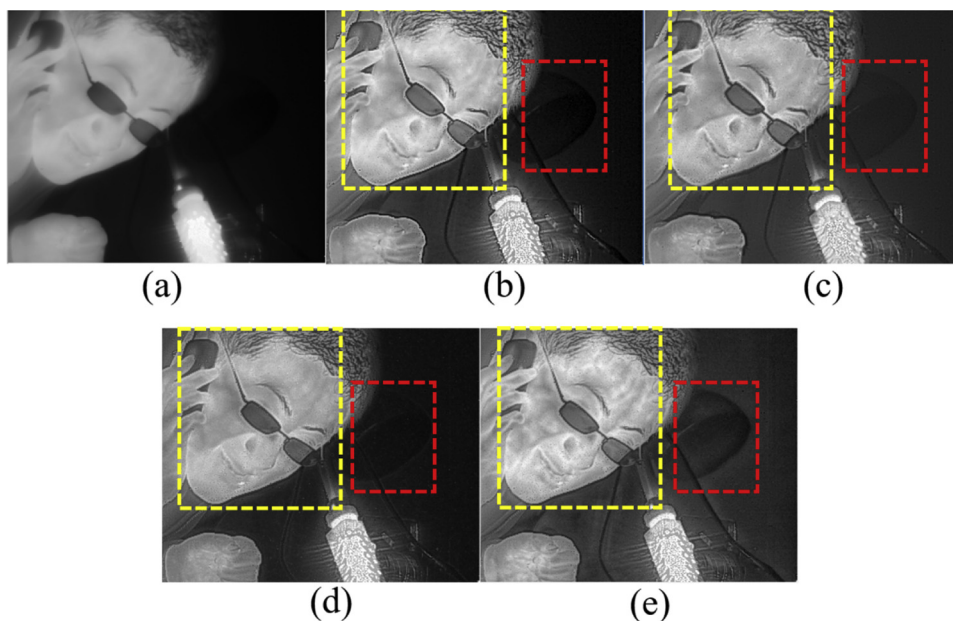


Fig. 8. Test set 4 of the enhancing performance. (a)the original image with normal histogram equalization; (b)detail enhancement with the bilateral filter; (c)detail enhancement with the guided image filter; (d)detail enhancement with the joint-bilateral filter; (e)detail enhancement of our new algorithm with BEEPS.

human face is extract more than the others.

Fig. 9 is the final visual comparison. As it can be seen, the red boxes show that our method can extract more detail and have better enhancing performance. Meanwhile, the yellow boxes show that, our algorithm can get rid of the shades by the enhancing effect.

All 5 figure comparisons give the same conclusion that, our new algorithm with the BEEPS has the best visual effect of the detail enhancement. The processed image looks much acceptable, the contrast is better mapped, the noise is strictly controlled.

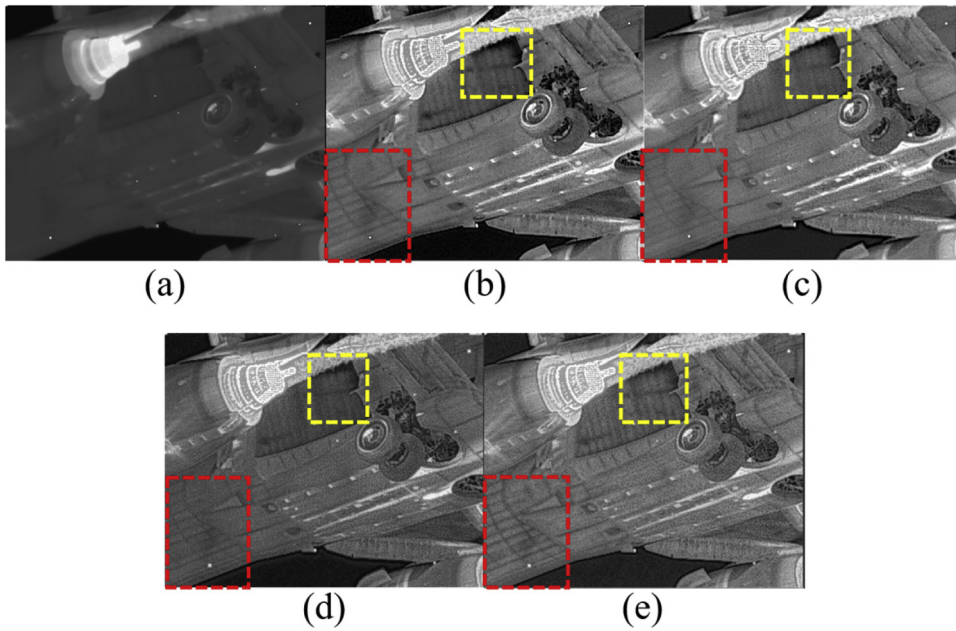


Fig. 9. Test set 5 of the enhancing performance. (a) the original image with normal histogram equalization; (b) detail enhancement with the bilateral filter; (c) detail enhancement with the guided image filter; (d) detail enhancement with the joint-bilateral filter; (e) detail enhancement of our new algorithm with BEEPS.

3.2. Computational time

Computational time is a very important index to evaluate whether an algorithm is applicable for industrial usage. We have mentioned that although we have successfully migrated the bilateral filter in the FPGAs for real-time application, it takes up too much on-chip rams and logic elements to deploy such big pipeline data structure. Also, the power consumption of the bilateral filter on the hardware is way too much, that means, this algorithm will not work well on low-level FPGAs. The guided image filter and the joint bilateral filter has the same problem. We test the computational time of all these 4 algorithms and find that, our new method has the best performance in reducing the computational time.

Fig. 10 shows that our new algorithm is way much faster than the other methods. The bilateral filter and the joint bilateral filter are way much slower because of their complicated convolutional calculation, also because of their non-linear nature. The guided

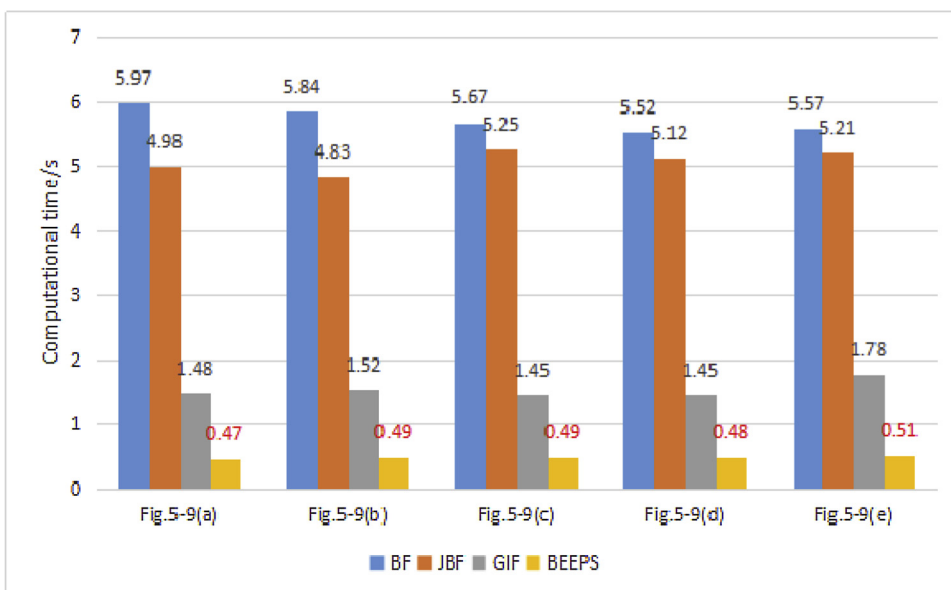


Fig. 10. The comparison of the computational time.

image filter is much better in computational time than the former two methods, although guided image filter has complex convolutional calculation too, its linear nature helps in reducing the computational time. However, it still cannot reach the level of our new algorithm, data shows that, the time-reducing effort of our new algorithm. The time has been reduced in orders of magnitude. According to the equations in section 2, the application of this new algorithm is basically an iterative calculation, no complex convolution kernel needs to be calculated during the process of the input images. The computational time of the whole algorithm only cares about the dimension of the input image, and leave the image data, parameter selection aside. This algorithm can be migrated into low and high-level FPGAs easily, and the power consumption will fall into a very satisfaction grade. The normal data operation procedure in the FPGA such as the Grid-methods process the image data stream with the look out table to speed up the 2D calculation. That means, when computing a target pixel value in the grid, all pixels within the grid. The computation will be take many times since the grid is a 2D form, thus, repeated calculation occurs. When dealing with a certain line of selected pixels, three lines of data must be flushed in the FPGA, the minim computational time is 192 μ s. This will be much longer with the expansion of the grids. In our method, 2D calculation has been simplified into 1D calculation, in which case, the calculation of the pixel within a selected line can be finished with only one line of data with a total 64 μ s at most, which is surely speed up the whole process.

3.3. Index comparison

In this section, we will compare the performances of our new algorithm with the latest proposed methods through some numerical indexes. We choose the Background Variation-Detail Variation(BV-DV) index and the Root-Mean-Square Contrast (RMSC) index to evaluate the performances of the selected algorithms.

The BV-DV index is used to evaluate the detail enhancement performance [10], it has a criterion to determine whether a pixel belongs to the “background” or the “detail”. If the gray value of a chosen pixel fluctuates less with the adjacent pixels, it will be marked as “background pixel”, otherwise, “detail pixel”. We calculate the BV index of all the determined background pixels and the DV of all the determined detail pixels of Fig. 5–9. The results are showed in Fig. 11 as follows:

According to Fig. 11, the BV-DV index mainly focus on the detail enhancement performance of the processed image. Then, we use the RMSC index to give another evidence of the contrast improvement. As we know, one character of the raw infrared image is that it has wide dynamic range. Usually in an raw infrared image, the low temperature object and the high temperature object have big span in gray scale. This can bring unacceptable contrast when display the raw image into 8-bit range. Thus, we choose the RMSC index to illustrate the modified contrast by numerical values, and prove the superiority of our new algorithm with the index values and the visual effects. The RMSC index can be calculated as follows:

$$RMSC = \sqrt{\frac{1}{M \times N} \sum_{i,j} (I(i,j) - \bar{I})^2} \quad (13)$$

where \bar{I} is the average gray value of the processed image. M and N are the number of rows and columns, respectively. By calculating the ambiguity of every processed pixel value with the image mean, the modified contrast of the processed image can be clearly illustrated. Larger RMSC value reflects larger contrast. The results are shown below (Fig. 12):

The BV-DV index and the RMSC index give us objective evidences that our new algorithm is superior than the other methods. In

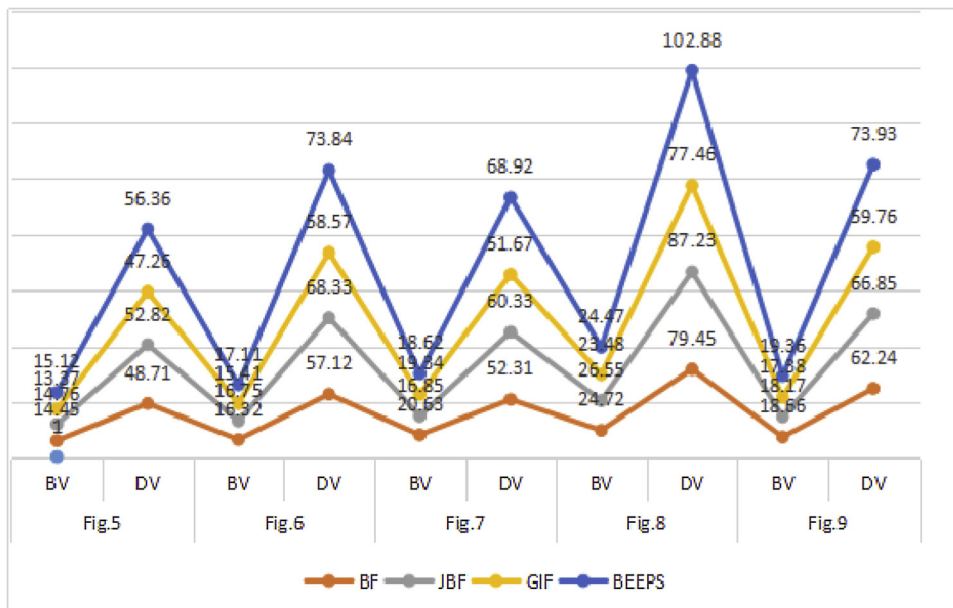


Fig. 11. BV-DV index comparison of Figs. 5–9.

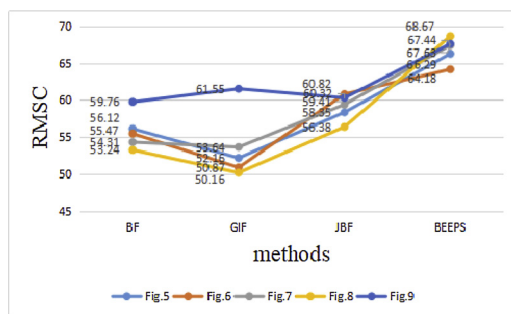


Fig. 12. RMSC index comparison of Figs. 5–9.

all 5 figures, the BV index are close because the base layers are nearly the same. However, the DV index fluctuates strongly with all five figures. This is because every edge-preserving method extracts different details and then enhances them. While in the RMSC index, the new algorithm has better value evidence, that is to say, the modified contrast of the improved image is much suitable for human observation.

4. Conclusion

In this paper, we proposed a new infrared image detail enhancement algorithm. This algorithm uses a bi-exponential called BEEPS to extract the detail information of an infrared image. Although the BEEPS is a non-linear filter, the computational time of our algorithm has been improved significantly. Visual effect and index test show that the new algorithm has superior advantages than the former raised detail enhancement algorithms. According to the test on the FPGAs, we believe that this algorithm will be widely applied in the real-world applications.

Acknowledgement

This work was supported in part by the National Science Foundation of China under Grant 61505083 and the Scientific Research Foundation of Nanjing University of Posts and Telecommunications (NO. NY215043).

References

- [1] J. Silverman, Display and enhancement of infrared images, *International Conference on Image Processing and Its Applications* (1992) 345–348.
- [2] T.H. Yu, Q.M. Li, J.M. Dai, New enhancement of infrared image based on human visual system, *Chin. Opt. Lett.* 7 (3) (2009) 206–209.
- [3] R. Lai, Y.T. Yang, B.J. Wang, H.X. Zhou, A quantitative measure based infrared image enhancement algorithm using plateau histogram, *Opt. Commun.* 283 (21) (2010) 4283–4288.
- [4] X.B. Bai, F.G. Zhou, B.D. Xue, Infrared image enhancement through contrast enhancement by using multiscale new top-hat transform, *Infrared Phys. Technol.* 54 (2) (2011) 61–69.
- [5] S.M. Pizer, E.P. Amburn, J.D. Austin, R. Cromartie, A. Geselowitz, T. Greer, B.T.H. Romeny, J.B. Zimmerman, Adaptive histogram equalization and its variations, *Comput. Vis. Graph. Image Process.* 39 (3) (1987) 355–368.
- [6] K. Zuiderveld, Contrast limited adaptive histogram equalization, *Graphics Gems IV*, Academic Press Professional, Inc., San Diego, 1994, pp. 474–485.
- [7] F. Branchitta, M. Diani, G. Corsini, A. Porta, Dynamic-range compression and contrast enhancement in infrared imaging systems, *Opt. Eng.* 47 (7) (2008) 076401.
- [8] C. Zuo, Q. Chen, N. Liu, Display and detail enhancement for high-dynamic range infrared images, *Opt. Eng.* 50 (12) (2011) 127401.
- [9] N. Liu, D.X. Zhao, Detail enhancement for high-dynamic-range infrared images based on guided image filter, *Infrared Phys. Tech.* 67 (2014) 138–147.
- [10] N. Liu, Xiaohong Chen, Infrared image detail enhancement approach based on improved joint bilateral filter, *Infrared Phys. Tech.* 77 (2016) 405–413.
- [11] N. Liu, The Research on Electronics Theory and Key Technology of Cooled Staring Infrared Detector and Simulated Detector, Ph.D Dissertation, (2013).
- [12] P. Thévenaz, D. Sage, M. Unser, Bi-exponential edge-preserving smoother, *Ieee Trans. Image Process.* 21 (2012) 3924–3936.
- [13] M. Elad, On the origin of the bilateral filter and ways to improve it, *IEEE Trans. Image Process.* 11 (2002) 1141–1151.
- [14] S. Paris, P. Kornprobst, J. Tumblin, P. Durand, Bilateral filtering: theory and applications, *Found. Trends Comput. Graph. Vis.* 4 (2008) 1–73.
- [15] G. Guarnieri, S. Marsi, G. Ramponi, Fast bilateral filter for edge-preserving smoothing, *Electron. Lett.* 42 (2006) 396–397.
- [16] B. Weiss, Fast median and bilateral filtering, *ACM Trans. Graph.* 25 (2006) 519–526.
- [17] S. Paris, F. Durand, A fast approximation of the bilateral filter using a signal processing approach, *Int. J. Comput. Vis.* 81 (2009) 24–52.
- [18] J. Shen, S. Castan, An optimal linear operator for edge detection, *Proc. IEEE Comput. Soc. Comput. Vis. Pattern Recognit.* Miami Beach, FL, June, 1986, pp. 109–114.